Gas Sorption in Poly(butylene terephthalate). II. Influence of Crystallinity and Molecular Orientation

Z. ZHOU, J. D. SCHULTZE, and J. SPRINGER*

Institut für Technische Chemie, Fachgebiet Makromolekulare Chemie, Technische Universität Berlin, Straße des 17. Juni 124, D-1000 Berlin 12, Germany

SYNOPSIS

Sorption measurements of CO_2, Ne, and Ar in poly(butylene terephthalate) (PBTP) films were studied by the gravimetric method with a recording microbalance at 298 K in the pressure range of 1–22 bar. The semicrystalline samples were annealed and oriented at 373 K. The sorption isotherms for CO_2 in PBTP films in the glassy state can be well described by the dual-sorption theory. The nonlinear sorption behavior of Ne and Ar can be satisfactorily analyzed using the sorption model developed for noble gases in PBTP. For the undrawn annealed films, it has been found that the increment of crystallinity leads to the reduction of the equilibrium gas concentration. For the oriented films, the gas concentration rises with increasing draw ratio. It appears that the sorption behavior for all tested gases in the oriented PBTP films does not depend on the changes of crystallinity and crystalline morphology under extension. The difference of the critical pressure p^* indicates the change in the size of the frozen microvoids existing in the noncrystalline phase, which was altered by annealing and drawing. © 1993 John Wiley & Sons, Inc.

INTRODUCTION

In general, phenomena concerning gas sorption in polymers below the glass transition temperature T_g can be successfully described by the dual-mode sorption model. This model consists of a contribution from a Henry's law term C_D, which also describes the gas sorption behavior in rubbery polymers, and a Langmuir adsorption term C_H.[1-4] According to this model, the equilibrium gas concentration C is given by

$$C = C_D + C_H = k_D p + \frac{C'_H b p}{1 + bp} \qquad (1)$$

k_D, C'_H, and b are the Henry's solubility constant, the Langmuir capacity, and the hole affinity constant, respectively, and p is the pressure of the penetrant gas.

However, in some gas/glassy polymer systems,[5-9] it was found that sorption isotherms must be reinterpreted in terms of an extension of the dual-sorption theory. It was pointed out that the plasticizing effect of sorbed gases exists in some gas sorption processes.[6-16] To describe the sorption behavior of penetrant/glassy polymer systems such as water vapor/poly(acrylonitrile), vinyl chloride monomer/poly(vinyl chloride) and ethane, as well as n-butane/poly(n-butyl methacrylate), the term C_D in an extension from Mauze and Stern[6,7,12] is modified as a stronger function of penetrant concentration or pressure than the commonly used dual-mode sorption model. Kamiya et al.[8] considered the effect of penetrant concentration on C_H for the CO_2/poly(vinyl benzoate) system.

Several investigations on the sorption of gases in semicrystalline glassy poly(butylene terephthalate) (PBTP) have been carried out in our laboratory.[17-20] The concentration of CO_2 was found to be significantly higher than that of Ne and of Ar. This was attributed to a specific interaction between CO_2 and PBTP. The sorption isotherm for CO_2 was analyzed by the dual-mode sorption model, whereas the sorp-

* To whom correspondence should be addressed.

Journal of Applied Polymer Science, Vol. 47, 13–20 (1993)
© 1993 John Wiley & Sons, Inc. CCC 0021-8995/93/010013-08

tion behavior of Ne and Ar did not obey to this model. Their sorption isotherms can be described by the sorption model developed for the noble gases in PBTP,[19] i.e., by

$$C = k_D p \qquad (0 < p \leq p^*) \tag{2}$$

and

$$C = k_D p + \frac{C'_H b(p - p^*)}{1 + b(p - p^*)} \qquad (p > p^*) \tag{3}$$

where p^* is the critical adsorption pressure. It depends mainly on the relative size of frozen microvoids and noble gas atoms. On the basis of this model, Henry's solubility occurs over the whole pressure range, while the additive Langmuir adsorption occurs only above p^*. The smaller the size of the noble gases compared to that of the frozen microvoids, the freer the gas molecules can move in the frozen microvoids and the higher the p^* obtained.

It is well known that two crystalline modifications (α- and β-form) exist in PBTP.[21–23] Under mechanical deformation, the transition between the two modifications takes place reversibly from the α-form to the β-form by elongation and inversely by relaxation. Besides, the semicrystalline PBTP has two spherulitic morphologies in the α-modification: usual and unusual spherulites.[24] The usual spherulites have a higher melting point than have the unusual ones. In the present work, we focused on the effect of the crystallinity and especially on the effect of the molecular orientation of PBTP on the gas sorption and transport. This involves several morphological changes of PBTP, e.g., crystallinity as well as noncrystalline and crystalline orientation. All these changes also vary the morphology of the noncrystalline, i.e., the permeable phase. Therefore, gas sorption and transport are affected. In the previously related investigations[25–33] of gas sorption and transport in oriented semicrystalline polymers, the altered behavior has been explained always on the basis of the changes of crystallinity and crystalline orientation. There was only little interest in the orientation behavior of noncrystalline regions.[34]

EXPERIMENTAL

Materials

The as-received PBTP films used in this study were free of additive commercial products. Platilon KF was supplied by Atochem Deutschland, Bonn, Germany. This transparent film had a thickness of 0.15 mm. It was used for preparation of all oriented and annealed samples.

The gases used in the sorption measurements, CO_2, Ne, and Ar, had a purity of 99.99%. They were obtained from Messer-Griesheim, Düsseldorf, Germany, and were used as received.

Sample Preparation

The preparations for all annealed and uniaxial drawn samples were done using an modified Instron 1026 tensile testing machine. The clamps modified to take up films were mounted in a chamber lined with insulation and containing heating elements coupled to a power regulator and temperature controller.

The samples were prepared by cutting rectangular strips of the as-received film. The sample was lightly clamped at both ends without load by the crosshead mechanism inside the chamber. The chamber was then heated quickly to the desired annealing temperature of 373 K and the sample was annealed at this temperature for 30 min. After annealing, the sample was immediately air-quenched to room temperature. In the case of extension, the samples were closely clamped to the crosshead inside the chamber. The direction of extension was perpendicular to that of the original machine direction of the as-received film. The annealing procedure for the drawn samples was the same as for the just annealed ones. Before quenching, the annealed sample was drawn with a crosshead speed of 50 mm/min. The sample was air-quenched to room temperature after drawing. Then, the oriented sample clamped by the crosshead was stored under extension load at room temperature for 3 days to complete the stress relaxation. After that, the oriented sample was taken out of the crosshead and stored for 3 additional days before the draw ratio λ was determined. The draw ratio was determined using the parallel ink lines along the transverse direction of the film. As the draw ratio was obtained by following additional ink lines drawn in the central region of the undrawn specimen at the last time before the characterization as well as sorption measurements, the reported draw ratios are actual and not nominal values. The different draw ratios of the samples extended at 373 K were $\lambda = 1$, 2, and 3, respectively. The samples for sorption measurements and physical characterization were all taken from the central sections of the annealed and oriented films.

Table I Physical Properties of PBTP Samples

Physical Data	As-received Sample	Annealed and Drawn Samples		
		$\lambda = 1$	$\lambda = 2$	$\lambda = 3$
X_{cw}^{D} (%)	21.7	32.3	31.5	32.3
X_{cw}^{T} (%)	30.2	37.6	37.3	38.6
T_g (K)	319	335	333	335
$\Delta n \times 10^3$	1.45	2.09	116	147
v_a	0.80	0.30	0.29	0.30

X_{cw}^{D} and v_a from density and X_{cw}^{T} from DTA measurements. Annealing and drawing temperature 373 K. T_g from dynamic mechanical investigations.

Physical Characterization

The annealed and drawn samples were transparent as were the as-received film. The densities of the samples were obtained by the density gradient column method using an aqueous calcium nitrate solution and factory-calibrated density glass beads at 296 K. According to the literature concerning the density of amorphous (1.256 g/cm^3)[35] and that of crystalline (1.396 g/cm^3) (α-modification)[24] PBTP, the mass related crystallinities X_{cw}^{D} were calculated. The obtained values are listed in Table I. Thermal analysis for all samples was performed by differential thermal analysis (DTA) using a Mettler TA 2000 thermoanalytic device in the temperature region between 223 and 533 K. The heating rate was 10 K/min. The sample weights were 7–10 mg; 14.5 mg of Al_2O_3 were used as reference. The melting temperatures of usual spherulites for as-received, annealed, and oriented samples lay almost at 498 K.[20] For the sample annealed at 373 K, a melting peak at about 385 K follows the glass transition. This endotherm peak involves the growth of unusual spherulites[24] that disappeared under extension at about $\lambda = 2$.[20] The calculated crystallinities X_{cw}^{T} based on a heat of fusion of 144.6 J/g for the crystals (α-modification)[36] are shown in Table I. As the β-modification whose density is about 1.283 g/cm^3 (Ref. 21) was present in the samples, it was not feasible to use the density method and the thermal analysis for determination of crystallinity of PBTP samples in which α- and β-modifications exist. Therefore, these results as well as those from density measurements are used only to analyze the change of crystallinity. The dynamic mechanical properties of the samples were measured by a dynamic torsional pendulum device, Zwick Torsiomatic 5203, at a heating rate of 2 K/min and a frequency of 1 Hz in the temperature region between 153 and 393 K. The glass transition temperatures T_g are given in Table I. The birefringence Δn of the sample was determined by a polarizing microscope, a Leitz Ortholux II Pol-Mk, equiped with a tilting compensator at room temperature. The results are also shown in Table I. Furthermore, the samples were characterized by wide-angle X-ray diffraction, Fourier transform infrared spectroscopy, and scanning electron microscopy.[20]

In the as-received semicrystalline film whose crystalline phase was unoriented, it was found that the major part of the crystals existed in the α-modification, while only a small part of the crystals was present in the β-modification, which was also found in the melt-quenched PBTP sample.[37] After annealing at 373 K, the crystallinity and the content of α-modification increased, while the content of β-modification decreased correspondingly. The slightly oriented chain segments in the amorphous phase were deoriented by annealing.[20] On starting of the uniaxial extension of the sample at 373 K, the unusual spherulites in the annealed samples were destroyed at small draw ratios. At the same time, the elastical deformation of the chain segments in the noncrystalline regions occurred. Following that, in the necking region, the lamellae as well as the usual spherulites were gradually transformed into fibrillar structure. This happened at the end of the plateau region of the stress–strain curve at a draw ratio of about $\lambda = 2$. At $\lambda = 3$, the perfect fibrillar structure was built.[20] The destruction of crystals led to the reduction of crystallinity and the β-modification content. Above $\lambda = 1.2$, the crystallinity and the β-modification content rose with increasing draw ratio.[20] But at $\lambda = 2$, the crystallinity is still lower than

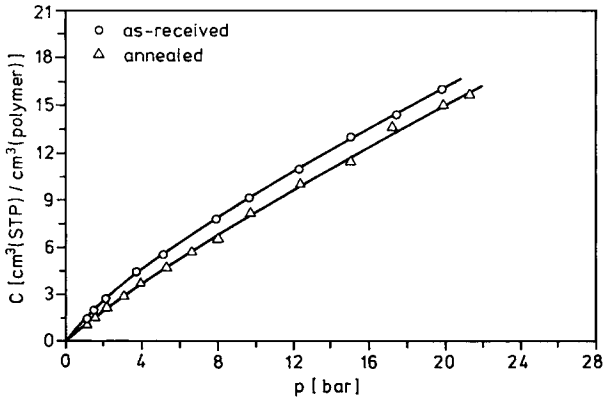

Figure 1 Sorption isotherms for CO_2 in PBTP films at 298 K. The lines were calculated from eq. (1) using parameters given in Table II.

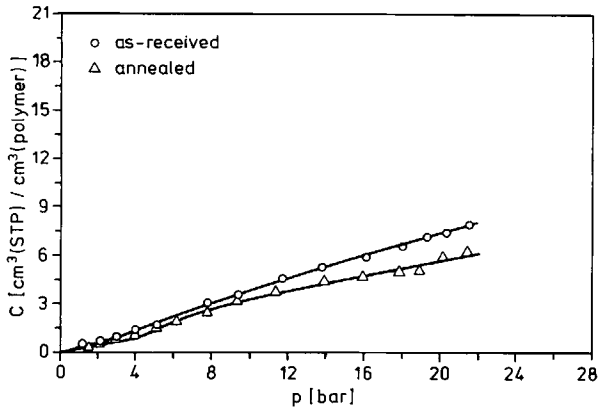

Figure 2 Sorption isotherms for Ne in PBTP films at 298 K. The lines were calculated from eqs. (2) and (3) using parameters given in Table II.

that at $\lambda = 1$. The orientation of the chain segments in the noncrystalline regions increased with draw ratio. Above $\lambda = 2$, the crystallization occurring in the oriented chain segments in these regions takes place.[20]

Sorption Measurements

The sorption isotherms for the gas/PBTP systems were obtained by a gravimetric sorption apparatus that consists mainly of a Sartorius Model 4436 electromicrobalance, encapsulated in a stainless-steel chamber, which permits the application of pressures up to 100 bar. Details about the description and operation of this device have been reported previously.[17,18]

The gas sorption measurements were carried out at 298 K in a pressure range of 1–22 bar. The sorption parameters were obtained by nonlinear least-square analysis according eqs. (1)–(3).

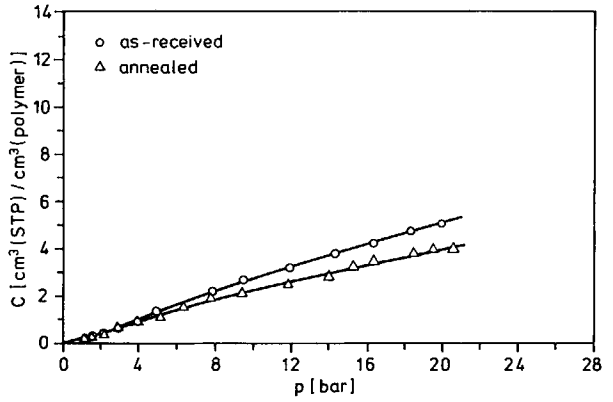

Figure 3 Sorption isotherms for Ar in PBTP films at 298 K. The lines were calculated from eqs. (2) and (3) using parameters given in Table II.

RESULTS AND DISCUSSION

Effect of Crystallinity on the Gas Sorption

The sorption isotherms for CO_2, Ne, and Ar in the as-received and annealed PBTP films are shown in Figure 1–3. One can easily see that the equilibrium concentrations for all gases in the annealed film are lower than that in the as-received film. We consider that the sorbing phase for gas is the noncrystalline region and the crystalline transition (α-modification $\rightleftarrows$ β-modification) does not affect the gas sorption behavior. However, the crystalline transition is involved with the change of crystallinity that influences the volume fraction of the noncrystalline phase as well as the number of the frozen microvoids.

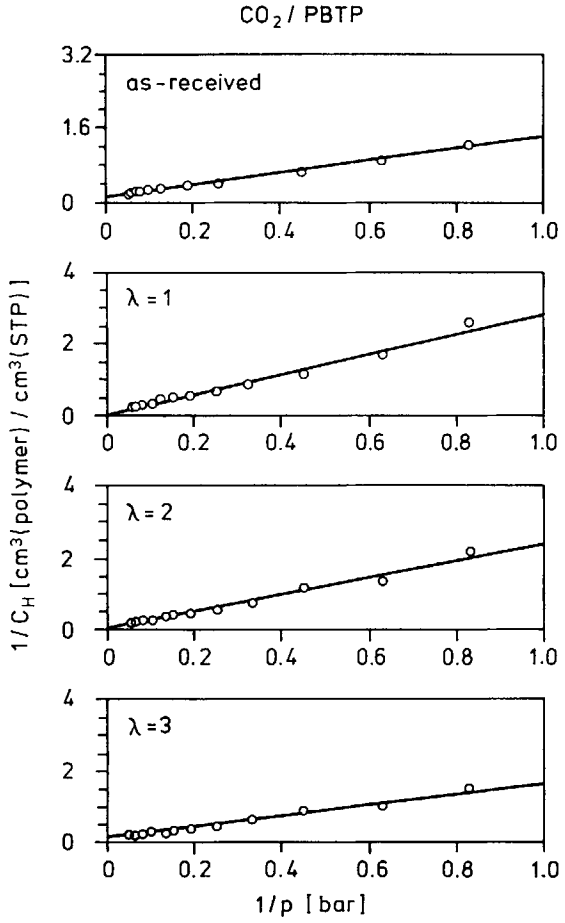

Figure 4 Test of the Langmuir equation for describing CO_2 sorption data. The lines were computed using parameters given in Table II.

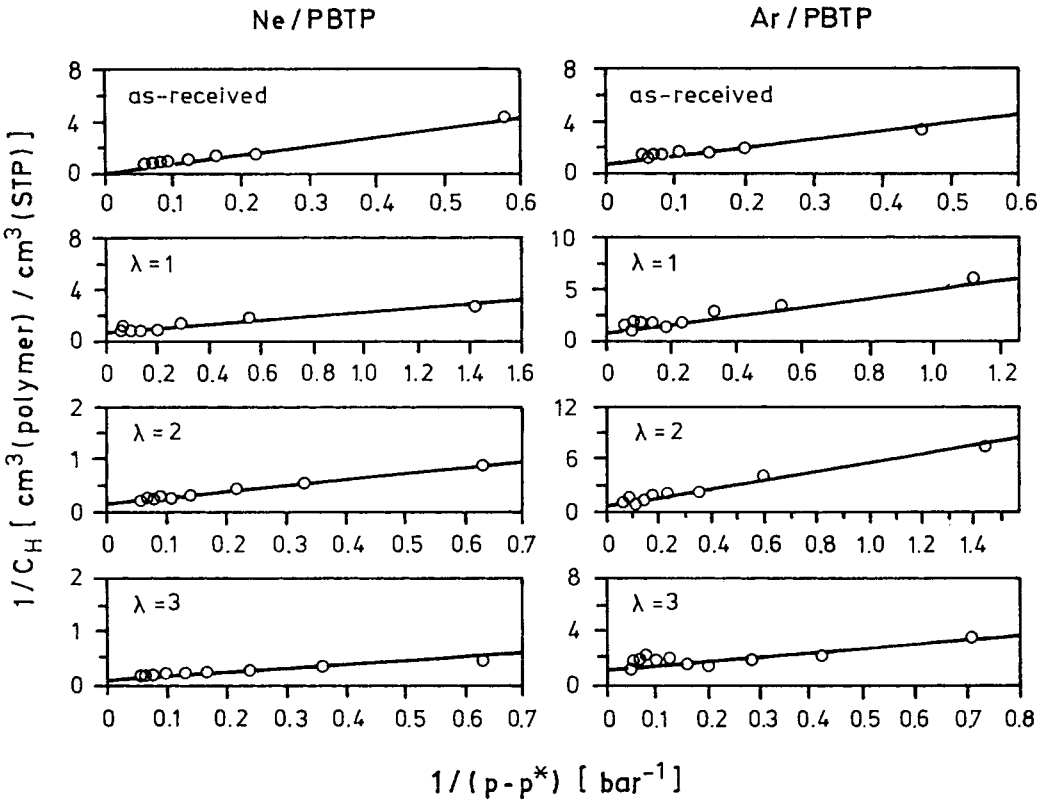

Figure 5 Test of the Langmuir equation for describing Ne and Ar sorption data. The lines were computed using parameters given in Table II.

The relative content of modifications (α- and β-forms) will not be considered here. The annealing of the samples led to an increment of crystallinity, which results in the reduction of the volume fraction of the sorbing, i.e., noncrystalline phase, and the number of the frozen microvoids, so that the concentrations for all gases have decreased.

The gas sorption isotherms in Figures 1–3 show the typical nonlinear character that is usually obtained in the glassy state. Like the sorption behavior in the as-received PBTP film,[19] the sorption isotherm for CO_2 in the annealed film can be analyzed by the dual-mode sorption model [eq. (1)], whereas the sorption behavior for Ne and Ar is satisfactorily described by the sorption model developed for the noble gases in PBTP [eqs. (2) and (3)].[19] The linear character of the plots $1/C_H$ vs. $1/p$ for CO_2 as well as $1/C_H$ vs. $1/p - p^*$ for Ne and Ar demonstrates

Table II Sorption Parameters k_D, C'_H, and b, and Critical Adsorption Pressures p^*

Gas	X^D_{cw} (%)	$k_D \times 10^1$ (cm³ [STP]/cm³ Polymer bar)	C'_H (cm³ [STP]/cm³ Polymer)	$b \times 10^1$ (bar^{-1})	p^* (bar)
Ne	21.7	2.94	2.42	0.86	3.3
	32.3	2.20	1.38	4.77	4.4
Ar	21.7	2.15	1.10	1.72	2.8
	32.3	1.62	0.94	2.64	2.1
CO_2	21.7	5.64	6.49	1.32	—
	32.3	5.56	6.34	0.71	—

T = 298 K, as-received and annealed PBTP films.

that a Langmuir adsorption process is reasonable (Figs. 4 and 5). The sorption parameters, k_D, b, and C'_H obtained by fitting the experimental data and the corresponding models are given in Table II. The computed critical adsorption pressures p^* for Ne and Ar are also shown in Table II.

It is interesting that the critical adsorption pressure p^* for Ne rises with crystallinity, while p^* for Ar drops slightly. The reason may be attributed to the great change of the size of the frozen microvoids that were accompanied by the morphological change of the PBTP matrix by annealing, although the volume fraction of the noncrystalline phase as well as the number of the frozen microvoids were decreased by crystallization. This can be found from the reduction of k_D as well as C'_H with crystallinity for all gases. The size of the certain microvoids in the noncrystalline phase may be enlarged by extension of a part of the chains that changed to the crystalline phase by crystallization. These microvoids strongly affect the adsorption of the smaller noble gases (here: Ne) and postpone the beginning of the Langmuir adsorption of the noble gases, i.e., the critical pressure p^* to higher pressures. According to the proposed sorption model, the smaller the size of the noble gases compared to that of the frozen microvoids in PBTP, the higher the p^*.

Gas Sorption in Oriented PBTP Films

The sorption isotherms for CO_2, Ne, and Ar in the oriented PBTP films at 298 K are shown in Figures 6–8. A similar gas sorption mechanism as in the as-received and annealed films is observed. The sorption isotherms for CO_2 in the oriented films are described by the dual-sorption theory [eq. (1)]. Those

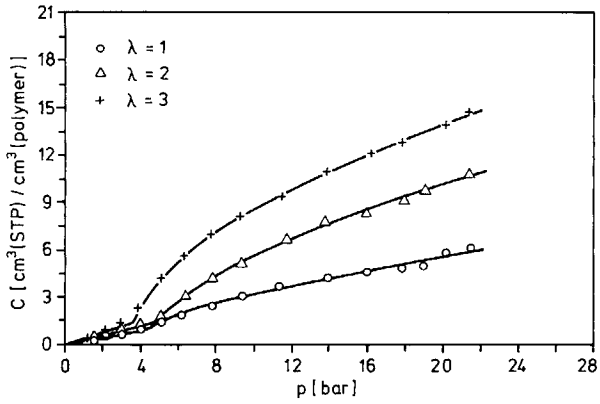

Figure 7 Sorption isotherms for Ne in oriented PBTP films at 298 K. The lines were calculated from eqs. (2) and (3) using parameters given in Table III.

for Ne and Ar can be analyzed by the sorption model for the noble gases in PBTP. The sorption parameters k_D, C'_H, and b as well as the critical adsorption pressures p^* for the noble gases obtained by the nonlinear least-square analysis are listed in Table III. The Langmuir plots show a linear dependence of $1/C_H$ on $1/p$ for CO_2 (Fig. 4) and of $1/C_H$ on $1/(p - p^*)$ for the noble gases (Fig. 5).

The gas concentrations presented in Figures 6–8 rise with increasing draw ratio. The Henry's solubility constants k_D and Langmuir capacities C'_H for CO_2, Ne, and Ar increase also with the draw ratio. It appears that the gas sorption behavior in the oriented PBTP films does not depend on the changes of crystallinity, crystalline orientation, and crystalline modifications. This phenomenon was also found for the CO_2 sorption in poly(ethylene terephthalate) films.[27] Vieth et al.[27] suggested a more revealing quantity C'_H/v_α, which may be viewed as the "frozen

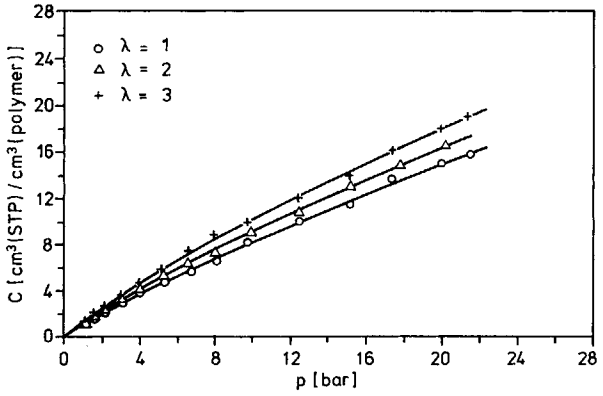

Figure 6 Sorption isotherms for CO_2 in oriented PBTP films at 298 K. The lines were calculated from eq. (1) using parameters given in Table III.

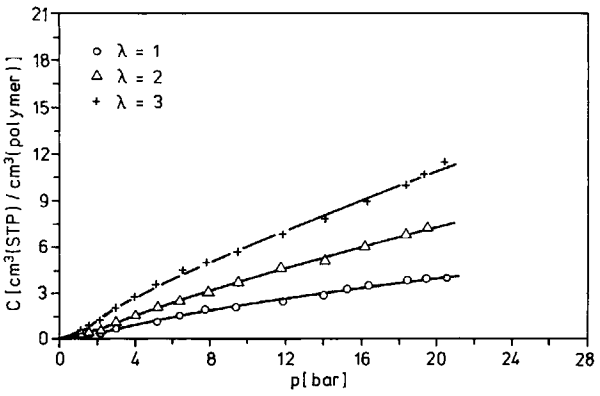

Figure 8 Sorption isotherms for Ar in oriented PBTP films at 298 K. The lines were calculated from eqs. (2) and (3) using parameters given in Table III.

Table III Sorption Parameters k_D, C'_H, and b and Critical Adsorption Pressures p^*

Gas	λ	$k_D \times 10^1$ (cm³ [STP]/cm³ Polymer bar)	C'_H (cm³ [STP]/cm³ Polymer)	$b \times 10^1$ (bar^{-1})	p^* (bar)	C'_H/v_a (cm³ [STP]/cm³ Polymer)
Ne	1	2.20	1.38	4.77	4.4	4.60
	2	3.10	5.45	1.64	4.8	18.79
	3	4.06	7.04	2.69	3.6	23.47
Ar	1	1.62	0.94	2.64	2.1	3.13
	2	3.19	1.16	1.72	2.3	4.00
	3	4.72	1.50	5.61	1.6	5.00
CO_2	1	5.56	6.34	0.71	—	21.13
	2	6.01	6.92	0.78	—	23.86
	3	6.49	7.19	1.00	—	23.97

T = 298 K, oriented PBTP films.

microvoids" saturation limit per unit volume of noncrystalline phase. v_α is the volume fraction of the noncrystalline phase (Table I). The C'_H/v_α values for CO_2, Ne, and Ar, given in Table III, show an increment with the draw ratio. It indicates a much larger sorption capacity in highly oriented films than in unoriented or slightly oriented films. As suggested by Vieth et al., it means that the orientation of the PBTP films under this extension condition tends to concentrate frozen microvoids in the residual noncrystalline phase. Besides, the tension process builds the relatively "loose" regions as well as the strained noncrystalline regions.[27] These "loose" regions in the noncrystalline phase tend to raise the gas solubility. The oriented noncrystalline morphology that increases the concentration with the draw ratio was certainly formed by the morphological transformation under extension. It is suggested that these noncrystalline regions may be almost formed by the destruction of the crystalline regions. There, the unusual spherulites were destroyed and the lamellae and usual spherulites were transformed into the fibrillar structure, because the chain segments in the primary noncrystalline phase were oriented with the draw ratio continuously so that they were formed into the strained noncrystalline regions, of which a part was transformed into the crystalline phase by orientation crystallization.

The effect of the relative size of the noble gas atoms and frozen microvoids on the sorption isotherms is obvious from Figures 7 and 8. The Langmuir adsorption of Ne in the oriented PBTP films occurs at a higher critical adsorption pressure p^* than for Ar. This seems to be reasonable as Ne is smaller than Ar. It is interesting to note that the critical pressures p^* for Ne und Ar have a maximum at $\lambda = 2$ and are lowest at $\lambda = 3$. It indicates that the size of the frozen microvoids has gone through a maximum with the draw ratio. This occurred in the process of transformation of lamellae as well as spherulites into the fibrillar structure. With the draw ratio and the formation of perfect fibrillar structure, the size of the frozen microvoids is strongly reduced, so that the critical pressure p^* is lowest at $\lambda = 3$.

As the changes of crystallinity, crystalline orientation, and α- and β-modifications have not shown an influence on the sorption behaviors in oriented PBTP films, the gas sorption in this oriented polymer depends only on the morphology of the noncrystalline phase.

CONCLUSIONS

The sorption behavior at 298 K for CO_2 in annealed and oriented semicrystalline PBTP films obeys the dual-sorption theory, whereas the sorption isotherms for Ne and Ar can be described by the sorption model developed for the noble gases in PBTP. In the unoriented films, annealed at 373 K, it is shown that the increment of crystallinity leads to the reduction of the equilibrium concentrations of CO_2, Ne, and Ar. The sorption isotherms for all gases in the oriented PBTP films rise with increasing draw ratio. They seem not to depend on the changes of crystallinity, orientation of crystals, and α-/β-phase ratio. The destruction of crystals, the transformation of lamellae as well as spherulites into the fibrillar structure, and the deformation of the samples under extension result in the change of the morphology of the noncrystalline phase. This would account for higher Henry's solubility constant k_D and Langmuir

capacity C'_H. The critical adsorption pressure determined from the experimental data allows us to estimate the change of size of the frozen microvoids in the noncrystalline phase of the PBTP films during annealing and drawing.

We kindly acknowledge the support of Dr. H. Cackovic with the X-ray diffraction measurements. One of the authors (Z. Z.) thanks the Technische Universität Berlin for financial support and is grateful to Dr. H. Springer for discussions. The Atochem Deutschland is thanked for providing the PBTP samples.

REFERENCES

1. R. M. Barrer, J. A. Barrie, and J. Slater, *J. Polym. Sci.*, **27,** 177 (1958).
2. A. S. Michaels, W. R. Vieth, and J. A. Barrie, *J. Appl. Phys.*, **34,** 1 (1963).
3. W. R. Vieth, J. M. Howell, and J. H. Hsieh, *J. Membr. Sci.*, **1,** 177 (1976).
4. W. J. Koros and D. R. Paul, *J. Polym. Sci. Polym. Phys. Ed.*, **16,** 1947 (1978).
5. V. Stannett, M. Haider, W. J. Koros, and H. B. Hopfenberg, *Polym. Eng. Sci.*, **20,** 300 (1980).
6. G. R. Mauze and S. A. Stern, *J. Membr. Sci.*, **12,** 51 (1982).
7. G. R. Mauze and S. A. Stern, *Polym. Eng. Sci.*, **23,** 548 (1983).
8. Y. Kamiya, T. Hirose, K. Mizoguchi, and Y. Naito, *J. Polym. Sci. Part B Polym. Phys.*, **24,** 1525 (1986).
9. R. J. Pace and A. Datyner, *J. Polym. Sci. Polym. Phys. Ed.*, **18,** 1103 (1980).
10. Y. Kamiya, K. Mizoguchi, Y. Naito, and T. Hirose, *J. Polym. Sci. Part B Polym. Phys.*, **24,** 535 (1986).
11. R. J. Pace and A. Datyner, *J. Polym. Sci. Polym. Phys. Ed.*, **19,** 1657 (1981).
12. S. A. Stern, U. M. Vakil, and G. R. Mauze, *J. Polym. Sci. Part B Polym. Phys.*, **27,** 405 (1989).
13. A. G. Wonders and D. R. Paul, *J. Membr. Sci.*, **5,** 63 (1979).
14. D. Raucher and M. D. Sefcik, ACS Symp. Ser. 223, American Chemical Society, Washington, DC, 1983, p. 89.
15. D. Raucher and M. D. Sefcik, ACS Symp. Ser. 223, American Chemical Society, Washington, DC, 1983, p. 111.
16. M. D. Sefcik and J. Schaefer, *J. Polym. Sci. Polym. Phys. Ed.*, **21,** 1055 (1983).
17. L. Phan Thuy and J. Springer, *Coll. Polym. Sci.*, **266,** 614 (1988).
18. J. D. Schultze, Z. Zhou, and J. Springer, *Angew. Makromol. Chem.*, **185/186,** 265 (1991).
19. Z. Zhou and J. Springer, *J. Appl. Polym. Sci.*, to appear.
20. Z. Zhou, Thesis D83, Technische Universität, Berlin, 1991.
21. M. Yokouchi, Y. Sakakibara, Y. Chatani, H. Tadokoro, T. Tanaka, and K. Yoda, *Macromolecules,* **9,** 266 (1976).
22. F. M. Lu and J. E. Spruiell, *J. Appl. Polym. Sci.*, **31,** 1595 (1986).
23. M. G. Brereton, G. R. Davies, R. Jakeways, T. Smith, and I. M. Ward, *Polymer,* **19,** 17 (1978).
24. R. S. Stein and A. Misra, *J. Polym. Sci. Polym. Phys. Ed.*, **18,** 327 (1980).
25. S. W. Lasoski and W. H. Cobbs, Jr., *J. Polym. Sci.*, **36,** 21 (1959).
26. A. S. Michaels, W. R. Vieth, and J. A. Barrie, *J. Appl. Phys.*, **34,** 1 (1963).
27. W. R. Vieth, H. H. Alcalay, and A. J. Frabetti, *J. Appl. Polym. Sci.*, **8,** 2125 (1964).
28. H. B. Hopfenberg and V. Stannett, in *The Physics of Glassy Polymers* (R. N. Haward, Ed., Elsevier, Amsterdam, 1972, Chap. 9.
29. C. E. Rogers, in *Polymer Permeability,* J. Comyn, Ed., Elsevier, London and New York, 1985, Chap. 2.
30. J. L. Williams and A. Peterlin, *J. Polym. Sci. Part A-2,* **9,** 1483 (1971).
31. R. E. Barker, R. C. Tsai, and R. A. Willency, *J. Polym. Sci. Polym. Symp. Ed.*, **63,** 109 (1978).
32. T. L. Wang and R. S. Porter, *J. Polym. Sci. Polym. Phys. Ed.*, **22,** 1645 (1984).
33. A. Peterlin, *Coll. Polym. Sci.*, **265,** 357 (1987).
34. M. J. El-Hibri and D. R. Paul, *J. Appl. Polym. Sci.*, **30,** 3649 (1985).
35. K. H. Illers, *Coll. Polym. Sci.*, **258,** 117 (1980).
36. M. Gilbert and F. J. Hybart, *Polymer,* **13,** 327 (1972).
37. W. Stach and K. Holland-Moritz, *J. Mol. Struct.*, **60,** 49 (1980).

Received November 22, 1991
Accepted February 14, 1992